

## Demonstration of a remote sensing/modelling approach for irrigation scheduling and crop growth forecasting

Katarzyna DĄBROWSKA-ZIELIŃSKA<sup>1)</sup>, M. Susan MORAN<sup>2)</sup>,  
Stephan J. MAAS<sup>3)</sup>, Paul J. PINTER Jr.<sup>2)</sup>, Bruce A. KIMBALL<sup>2)</sup>,  
Tom A. MITCHELL<sup>2)</sup>, Thomas R. CLARKE<sup>2)</sup>, Jianguo QI<sup>2)</sup>

<sup>1)</sup> Institute of Geodesy and Cartography, Remote Sensing Centre, Warsaw, Poland

<sup>2)</sup> USDA-ARS U.S. Water Conservation Laboratory, Phoenix, Arizona, USA

<sup>3)</sup> USDA-ARS Cotton Research Centre, Shafter, California, USA

**Abstract:** The PROtype Biomass and Evaporation (PROBE) model was developed for simulation of daily plant growth and evaporation ( $E$ ) rates in natural, vegetated ecosystems (MAAS *et al.*, 1992). The inputs to the model are basic meteorological information and periodic (weekly or bi-weekly) measurements of green leaf area index ( $GLAI$ ) and  $E$ . The model uses an interactive approach with two submodels – a vegetation growth (VG) submodel and soil water balance (SWB) submodel – where the estimate of  $GLAI$  from the VG submodel is used in the SWB submodel to calculate  $E$ . In turn, the estimate of  $E$  is used in a rerun of the VG submodel to refine the estimate of  $GLAI$ . This model was tested based on meteorological data and measurements of  $GLAI$  and  $E$  acquired in a cotton (*Gossypium hirsutum* L.) field in central Arizona. Overall, the modelled and measured values of  $GLAI$  and  $E$  corresponded well. Results showed that the time and precision of input data were very important to obtaining accurate estimates of  $GLAI$  and  $E$ . The model showed promise for use in scheduling crop irrigations.

**Key words:** PROBE model, evaporation,  $GLAI$ , soil water balance, crop growth forecasting

### INTRODUCTION

Production of agricultural crops in the arid and semiarid areas of the world is almost totally dependent on irrigation and, in humid areas, irrigation is increasingly used to supplement rainfall. Nevertheless, farmers are still searching for ways to determine the most beneficial time to apply just the right amount of water (termed “irrigation scheduling”). Accurate irrigation scheduling is in the interests of everyone since over-watering can result not only in decreased profits for the farmer but also in pollution of local ground water sources.

One conventional irrigation scheduling method is based on measurements of reference evaporation ( $E$ ) rates and crop coefficients. Reference  $E$  is defined as a rate at

which water, if available, would be removed from the soil and plant surface of a specific crop called the reference crop and is generally provided to farm managers by local agricultural meteorological networks. Crop coefficients ( $K_c$ ) are the ratios of evaporation of a specific crop to reference evaporation that have been derived from experimental data. The change in crop coefficient during the crop growing cycle is called a crop curve. The crop curve and crop reference  $E$  are used to monitor daily evaporative water loss within each cropped field to determine the optimum irrigation schedule. Though this method provides a means of determining where to irrigate and how much water to apply, it assumes that the crop is growing at the potential rate and does not account for such phenomena as within-field differences in soil type, insect infestations, and nonuniformity in water, pesticide and nutrient applications.

A variety of crop models have come out from the "School of de Wit". One of the first crop simulation model was ELCROS (Elementary CROp Simulator), (de WIT *et al.*, 1970), the model was followed by other models which included more than only meteorological data (FEDDES *et al.*, 1978; de WIT, 1987). ARKIN *et al.*, (1977) and HODGES (1977) performed the first use of remotely sensed information to crop growth models.

MAAS *et al.* (1992) proposed a new method based on a combined remote sensing/modelling approach designed to monitor actual (not potential) plant evaporative water loss. They proposed a plant growth simulation model with a simple soil water balance equation to simulate both plant biomass production and evaporation. This model required only the meteorological inputs necessary to compute reference  $E$  (mean daily air temperature, total daily solar radiation, mean relative humidity, daily mean wind speed) and general information about vegetation. The outputs of the model were plant biomass, green leaf area index ( $GLAI$ ), soil moisture and actual  $E$ . Periodic remotely-sensed estimates of  $GLAI$  and  $E$  were used to supplement the model, thus increasing accuracy and accounting for such unexpected events as insect. This combined approach proved successful for estimation of  $GLAI$  and daily  $E$  rates from an alfalfa field near Phoenix Arizona (MORAN *et al.*, 1995).

This report presents results from an application of the PROBE (PROtotype Biomass and Evaporation) model to cotton (*Gossypium hirsutum* L. cv. 'Deltapine 20') at the Maricopa Agricultural Centre (MAC), 30 miles south of Phoenix Arizona. The objectives of the study were to 1) refine the model for application to cotton, 2) run the model over the entire cotton growing season, and 3) compare modelled estimates of cotton  $GLAI$  and  $E$  with on-site field measurements. Model simulations were run to 1) determine the frequency, timing and precision of remotely-sensed measurements needed to maintain accurate output values, and 2) examine the potential of PROBE for biomass forecast and irrigation scheduling.

## EXPERIMENT

An experiment entitled Multispectral Airborne Demonstration at Maricopa Agricultural Centre (MADMAC) was conducted during the summer growing season in Arizona 1994 (MORAN *et al.*, 1996). MADMAC was designed to investigate the utility of remotely sensed data for day-to-day farm management. We acquired images in four spectral wavelength bands (green, red, near- IR and thermal) periodically during the cotton growing season (April to October) at MAC using airborne cameras flown at two altitudes (1200 and 2300 m) above ground level (AGL) for obtaining different size and scale of test area. Image frames were mosaiced to provide seamless images of MAC with 2 m spatial resolution for each date of overpass (Tab. 1). However, information from these images was not applied in this article and we used ground measurements synchronised with the acquisition of remote sensing data.

**Table 1.** Dates of aircraft overpasses during the MADMAC Experiment and derived estimates of *GLAI*, *E* and crop stage/status on those dates

DOY	<i>GLAI</i>	<i>E</i>	Crop Growth Stage and Status
165	0.20	7.80	vegetative, 10 % cover
187	1.61	9.03	vegetative, 50 % cover
193	3.89	11.24	flowers, 85 % cover
202	3.32	6.85	flowers, 80 % cover
214	3.33	9.30	green bolls, 80 % cover
223	3.32	10.03	green bolls, visible leaf wilting
228	3.32	11.15	green bolls, some insect infestation
235	3.32	5.01	mature bolls, heavy leaf perforator damage
243	3.32	2.04	mature bolls, severe leaf perforator damage

MAC, owned and operated by the University of Arizona, is a 770 ha farm located about 48 km S of Phoenix. A 1.5 ha cotton field (#116) at MAC was chosen for demonstration of the PROBE model. This field was centrally located within MAC, allowing sufficient fetch for meteorological measurements. However, it was a smaller field and did not receive the aerial insecticide sprays applied to the larger, more distant fields; this resulted in some insect damage to the crop, especially near the end of the season. Nonetheless, the cotton in Field 116 was flood irrigated on a regular basis, like all other cotton fields in the region. The farm management staff at MAC kept records of farm management practices such as irrigation amounts and timing, fertiliser and pesticide applications, cultivation practices, insect infestations, planting/harvest times and crop phenology. Each week, we measured such plant parameters as *GLAI*, percent cover, plant height and biomass of selected cotton fields at MAC. Five plants were weighed in each sample site and the plant of median weight was taken to the laboratory for measurement of wet and dry biomass and *GLAI*. The weight of the wet bio-

mass was measured immediately, dry biomass weight was measured after 48 hours in an oven at 68C, and *GLAI* was measured using a light-sensitive leaf area meter. During each aircraft overpass, we made an ocular estimate of the percent cover and plant height of all cotton fields, including Field 116.

A Bowen-ratio device was installed in the centre of Field 116 with instrumentation to measure hourly values of net radiation, soil heat flux (Radiation Energy Balance Systems, Seattle, Wash.; Model Q6 for net radiometer and HFT-3 for soil heat flux plates) and the Bowen ratio (Campbell Scientific, Logan, Utah) throughout the growing season. There was also an onsite Arizona meteorological station – AZMET (BROWN, 1989) providing hourly values of solar radiation, wind speed, air temperature, and vapour pressure throughout the year.

## THE MODEL

The submodels of the PROBE model have been described in detail by MAAS *et al.* (1992) and MORAN *et al.* (1995) and the model “calibration” procedure used to incorporate the remotely sensed data has been described by MAAS (1993a,b). The description of PROBE given here is sufficient for understanding this application and focuses primarily on the refinements made to convert the model application from alfalfa to cotton.

The PROBE model is based on the concept that field  $E$  is determined by the degree to which the  $E$  of the vegetation canopy approaches potential  $E$  ( $E_p$ ) and the degree to which the vegetation canopy covers the region. Hence, the PROBE model uses two submodels – a soil water balance submodel and a vegetation growth submodel – to estimate the available soil water fraction in the rooting zone ( $f_{sw}$ ) and the change in *GLAI*, respectively. With this information and a basic understanding of the relation between  $E/E_p$  and  $f_{sw}$  and *GLAI*, daily  $E$  was computed in PROBE using the following relationship

$$E = E_p F_{sw} F_{GC} \quad (1)$$

in which  $F_{sw}$  is the ratio  $E/E_p$  from Fig. 1A (ROSENTHAL *et al.*, 1987) and  $F_{GC}$  is the ratio  $E/E_p$  from Fig. 1B (RITCHIE, BURNETT, 1971).  $E_p$  was computed from routinely-available meteorological observations (average daily air temperature, average daily dew point temperature, average daily wind speed and total daily solar irradiance) using the combination equation described and validated by Van BAVEL (1966).

Eq. (1) was formulated to be simple, with the assumption that it would be updated with periodic  $E$  and *GLAI* measurements. As such, under certain conditions [e.g., when the field is flooded ( $F_{sw} \sim 1.0$ ) and the crop is immature ( $F_{GC} < 1.0$ )],  $E$  will necessarily be estimated to be less than  $E_p$ , even though on-site measures of  $E$  using conventional means, such as Bowen ratio, would estimate  $E = E_p$ . This is because Eq. (1) is a meas-

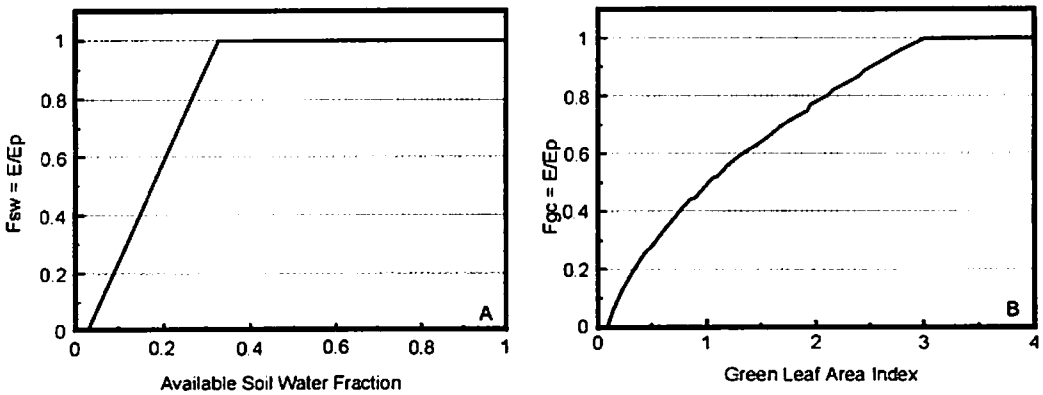


Fig. 1. Relations between the ratio  $ET/ET_p$  and A) available soil water fraction (ASWF) and B) green leaf index (GLAI)

ure of water loss from the rooting zone and neglects evaporation from the soil surface. On the other hand, under typical conditions (when the soil surface is dry or when the crop is near full-cover), Eq. (1) properly represents the dynamics of crop water flux. This concept will be revisited when the modelled estimates of  $E$  ( $E_m$ ) are compared to measured by the Bowen ratio apparatus ( $E_{BR}$ ) in later sections.

The PROBE model computes changes in soil water and  $E$  on a daily time step using the stepwise process depicted in Fig. 2. Daily values of  $GLAI$  for evaluating  $F_{GC}$  were obtained from the vegetation growth submodel. An initial amount of soil water was specified at the start of the simulation and, with each irrigation,  $F_{SW}$  was reset to 1.0 based on the assumption that the flood irrigation filled the soil profile to field capacity.

The formulation of the vegetation growth submodel is similar to that used in earlier agricultural crop growth models (MAAS, 1992; MAAS *et al.*, 1989). Photosynthetically active radiation ( $PAR$ ) was assumed to comprise 45 % of the total daily solar irradiance (BROWN, 1969).  $PAR$  absorbed by the vegetation canopy ( $APAR$ ) was computed using the relationship

$$APAR = PAR [1 - e^{-k(GLAI)}] \tag{2}$$

where  $k$  is the extinction coefficient (CHARLES-EDWARDS *et al.*, 1986). Production of new biomass ( $\Delta B$ ) and increase in  $GLAI$  ( $\Delta GLAI$ ) were determined using the relationships

$$\Delta B = APAR \epsilon f(T_a) \tag{3}$$

and

$$\Delta GLAI = \Delta B f A_{SL} \tag{4}$$

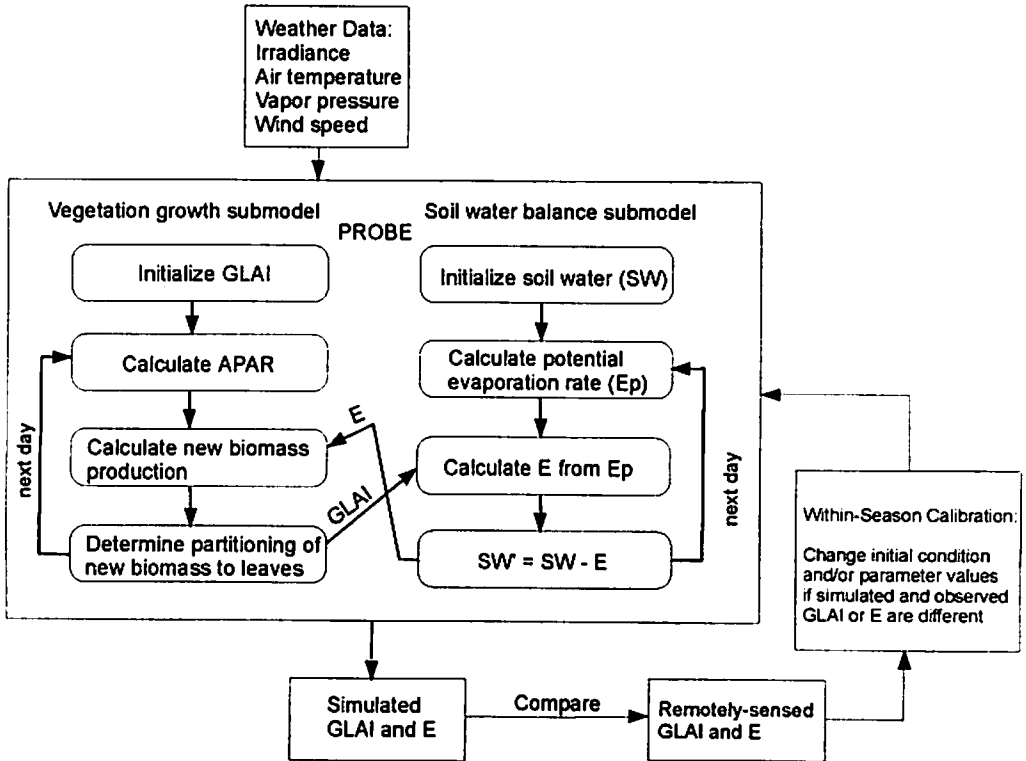


Fig. 2. Sequence of steps in computing  $E$  and  $GLAI$  within the PROBE soil water balance (SWB) and vegetation growth (VG) submodels and the iterative calibration procedure

where the parameter  $\epsilon$  is the “energy conversion efficiency” (CHARLES-EDWARDS *et al.*, 1986) and  $f(T_a)$  is a function that reduces the rate of biomass production at suboptimum air temperatures ( $T_a$ ). New leaf area ( $\Delta GLAI$ ) in the canopy was determined by partitioning a model-derived fraction of  $\Delta B$  to leaf biomass (leaf partitioning fraction –  $f_p$ ) and multiplying this quantity by the specific leaf area ( $A_{SL}$ , the  $m^2$  of leaf area per kg of leaf biomass) of the vegetation. On the day of its formation, new leaf area is assigned a lifespan in terms of accumulated degree-days that determines how long it will live prior to senescence from the vegetation canopy. The submodel maintains a running total of degree-days (computed from average daily air temperature) to determine what portion of the canopy leaf area is alive or dead on any given day of the simulation. If the calculated age of a leaf is greater than the lifespan, then that leaf tissue is considered to have senesced from the canopy and the dry mass associated with senescence is subtracted from the accumulated above ground dry mass.

For this cotton variety, the observed  $GLAI$  values for a long period did not decrease and the default parameter, which controls the leaf lifespan, was specified high. The leaf-partitioning fraction ( $f_p$ ) which controls the production of new leaf area was taken to be 0.47, the specific leaf area ( $A_{SL}$ ) was assumed to be  $0.015 m^2 \cdot g^{-1}$ . The ini-

tial condition for soil water content was estimated to be 150 mm, the extinction coefficient ( $k$ ) for cotton was 0.45, and the energy conversion efficiency ( $\epsilon$ ) was  $1.63 \text{ g-MJ}^{-1}$ . These coefficients were estimated based on tests of the model for potential growth of this cotton species under conditions at MAC.

An iterative numerical procedure (MAAS, 1993b) is built into the PROBE model to manipulate the initial conditions and/or parameters so that they converge on values that result in the model simulation fitting the set of remotely sensed estimates (Fig. 2). Periodic estimates of  $E$  were used to calibrate the soil water balance submodel and periodic estimates of  $GLAI$  were used to calibrate the vegetation growth submodel. In the soil water balance submodel, the initial value of soil water and the value of field capacity were manipulated to bring the  $E$  simulation into agreement with the corresponding observations. In the vegetation growth submodel, the initial value of  $GLAI$ ,  $f_p$ , and the value of the parameter responsible for leaf lifespan were manipulated to bring the  $GLAI$  simulation into agreement with the corresponding observations.

In simulating evaporation and biomass production using this model, the vegetation growth submodel was accessed first and calibrated using the remotely sensed  $GLAI$  estimates. The resulting set of simulated daily  $GLAI$  values were then used in an iteration of the soil water balance submodel, which was calibrated using the remotely sensed  $E$  estimates. Then, the vegetation growth submodel was rerun to incorporate estimates of ( $F_{sw}$ ) in the simulation of  $GLAI$  and biomass, where

$$\Delta B' = APAR \epsilon f(T_d) F_{sw} \quad (5)$$

and

$$\Delta GLAI' = \Delta B' f_p A_{SL} \quad (6)$$

## METHODS AND RESULTS

The PROBE model was run for the cotton in Field 116 based on meteorological data (average daily air temperature, average daily dew point temperature, average daily wind speed and total daily solar irradiance) obtained from the local AZMET station (BROWN, 1989). Since spectral data from MADMAC were not available at this time, we chose to conduct this demonstration of the PROBE model with periodic on-site estimates of  $E$  and  $GLAI$ , rather than remotely sensed estimates. This was a reasonable approach since the objectives of this analysis were to test the performance of the model for cotton, and to evaluate the sensitivity of the model to the frequency and timing of remotely sensed inputs. Thus, values of  $GLAI$  and  $E$  for supplementing the PROBE model runs were taken from on-site measurements as described in the next two sections. Though  $GLAI$  and  $E$  data were available for nearly every day of the experiment, we used only the values corresponding to the days of aircraft overpasses

(Tab. 1) for input to PROBE. This was done to simulate the frequency and timing of inputs under normal conditions.

### DERIVED *GLAI*

*GLAI* measurements were made in several of the large cotton fields during MADMAC, but not in Field 116. However, for all MAC fields, a drive-by, visual estimation of plant height and fractional vegetation cover was made during each over-pass listed in Tab. 1. In order to estimate *GLAI* of Field 116, we derived a relation between measurements of *GLAI* and plant cover (*CP*) for selected MAC cotton fields (Fig. 3A), where

$$GLAI = -1.23 + 5.69CP \quad (7)$$

with  $r^2 = 0.97$  and standard error 0.29. Eq. (7) was then used with the periodic visual estimates of *CP* in Field 116 to derive values of *GLAI* for Field 116 (Fig. 3B). All subsequent references comparing *GLAI* of Field 116 with model output actually refer to

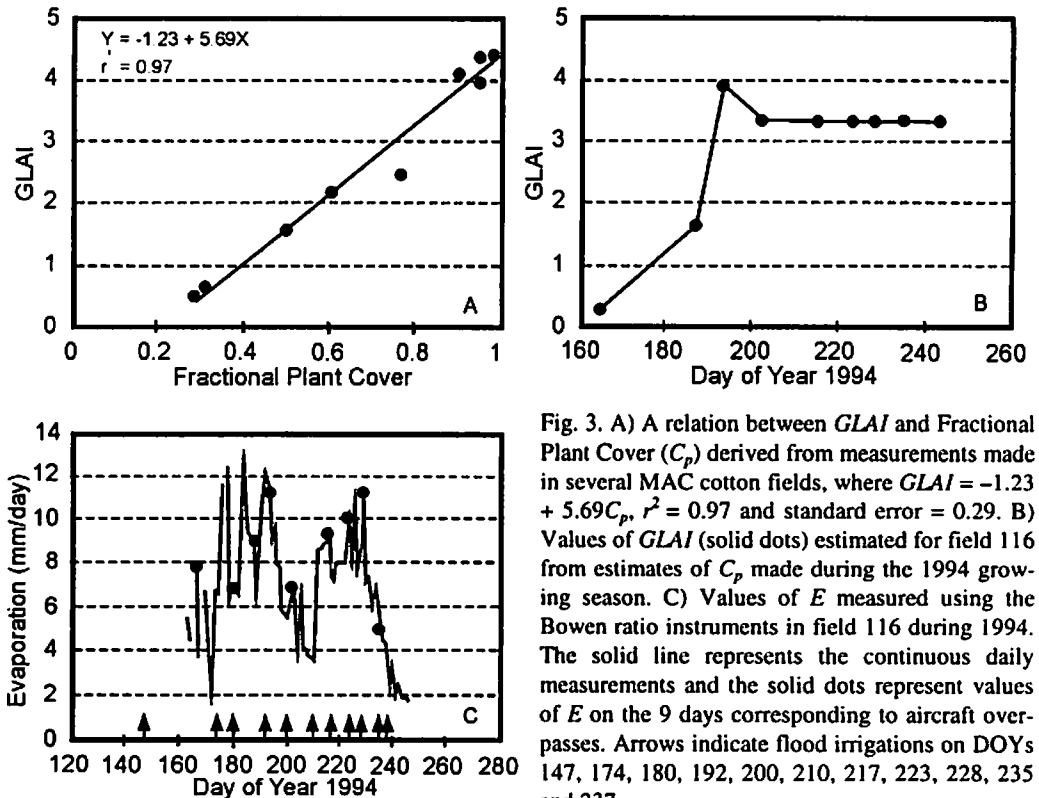


Fig. 3. A) A relation between *GLAI* and Fractional Plant Cover ( $C_p$ ) derived from measurements made in several MAC cotton fields, where  $GLAI = -1.23 + 5.69C_p$ ,  $r^2 = 0.97$  and standard error = 0.29. B) Values of *GLAI* (solid dots) estimated for field 116 from estimates of  $C_p$  made during the 1994 growing season. C) Values of  $E$  measured using the Bowen ratio instruments in field 116 during 1994. The solid line represents the continuous daily measurements and the solid dots represent values of  $E$  on the 9 days corresponding to aircraft over-passes. Arrows indicate flood irrigations on DOYs 147, 174, 180, 192, 200, 210, 217, 223, 228, 235 and 237

*GLAI* derived from these visual estimates of cover. As such, it will be termed “derived *GLAI*” rather than “measured *GLAI*”.

The cotton grown in Field 116 was infested with cotton leaf perforator (*Bucculatrix thurberiella*) just before reaching maturity near DOY 214. The leaf perforator larvae consume the succulent cotton leaf tissue between the leaf surfaces, leaving behind the dried epidermis of one side of tire leaf. Thus, the outside dimension of the leaf doesn't change much, but the effective *GLAI* and transpiring tissues can be reduced to near zero. In Field 116, infestation occurred before *CP* reached 100 % (DOY 230) and, by DOY 250, the entire canopy was infected and the crop was decimated. This caused our derived estimates of *GLAI* after DOY 230 to be higher than the actual *GLAI* because our visual estimates of *CP* were for total vegetation cover not green vegetation cover.

## MEASURED *E*

Though the planting date of the cotton was day of year (DOY) 102, the Bowen ratio measurements didn't begin until DOY 165 and then ran continuously through DOY 246. Flood irrigations were made on DOYs 147, 174, 180, 192, 200, 210, 217, 223, 228, 235, and 237 (see arrows in Fig. 3C). Over the growing season, *E* increased with the increase in *GLAI* and decreased shortly after the last irrigation and *GLAI* observation (DOY 243). *E* increased on the day of each irrigation and then declined steadily until the next irrigation. There were other more subtle trends in the data related to such meteorological conditions as high winds, cloudy skies and high air temperatures. Because of the frequent irrigations, evaporation rates were near potential for most of the growing season.

## MODELLED *GLAI* AND *E*

The PROBE model was tested under typical data-acquisition conditions. That is, we used the measured *E* and derived *GLAI* values on each overpass day, starting on the first day of available Bowen ratio data. This resulted in 9 values of *E* and *GLAI* for the days designated in Tab. 1, with a time interval between available *E* and *GLAI* inputs ranging from 5 to 22 days. As described in previous sections and Fig. 2, the model works in an iterative fashion beginning with an estimation of *GLAI* refined by intermittent inputs of *GLAI*, assuming *E* is at potential. Then, *GLAI* is used as an input to the soil water balance submodel to compute actual *E* and, subsequently, the vegetation submodel is rerun using Eq. (5) and (6). The results of these intermediate steps are presented in Fig. 4a-4e.

*GLAI* and biomass data presented in Fig. 4A (solid lines) are the results of the first vegetation simulation based on the vegetation submodel, the intermittent values of *GLAI* (squares), and the assumption that  $E = E_p$ . The modelled best fit showed a slow

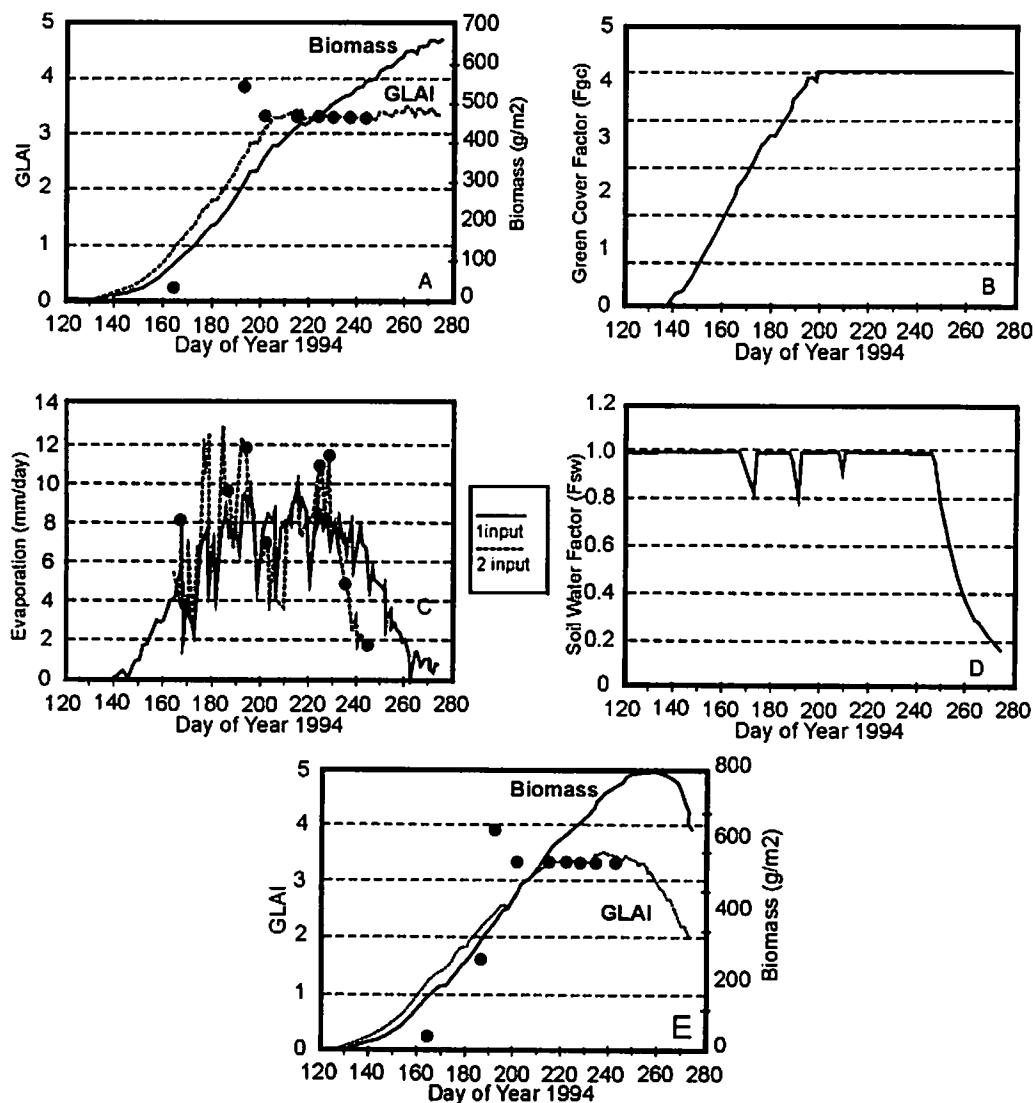


Fig. 4. A) Estimates of  $GLAI$  (dot line) and biomass (bold line) based on the first run of the vegetation submodel (assuming  $E = E_p$ ); the solid dots represent the input  $GLAI$  values. B) The Green Cover Factor ( $F_{GC}$ ) computed by PROBE indicating the increase from 0.0 near the time of emergence to 1.0 near the time of full vegetation cover (DOY 200). C) Values of  $E$  computed with PROBE (bold line), measurements of  $E$  with the Bowen ratio instruments (dot line) and input values of  $E$  (solid dots). D) The Soil Water Factor ( $F_{sw}$ ) computed by PROBE, where deviations from 1.0 occurred immediately before irrigations and at the end of the season. E) Estimates of  $GLAI$  (dot line) and biomass bold line based on the second run of the vegetation submodel, which incorporated values of  $F_{sw}$ ; solid dots represent the input  $GLAI$  values

growth pattern, but ever-increasing values of *GLAI* and biomass as could be expected for a healthy crop. The  $F_{GC}$  increased steadily from 0.0 near the time of emergence to 1.0 on DOY 200, near the time of 80 % vegetation cover (Fig. 4B). The mean absolute difference (MAD) between the derived and modelled values of *GLAI* for the 9 overpass days was on average of 0.32. High MAD values (0.74 and 0.54) occurred early in the season as the PROBE model attempted to fit the steep rise in *GLAI* values from DOY 187 to 202. The highest error (MAD value 1.29 on DOY 193) was possibly due to error in derived *GLAI* value, since it was substantially higher than the values on DOY 202 and thereafter.

The next stage in the PROBE simulation was to compute values of  $E$  based on the soil water submodel, computations of  $E_p$ , intermittent values of actual  $E$  ( $n = 9$ ), and the daily *GLAI* values simulated by the vegetation submodel. In the early season, crop cover increased steadily from 0 to about 80 % cover ( $F_{GC}$  1.0 on DOY 200) resulting in a steady increase in values of  $E$ , with minor fluctuations due to irrigations and weather conditions (Fig. 4C).  $E$  started to decline slightly after DOY 217 due to insect infestation and senescence, and declined rapidly after the last irrigation on DOY 237 and last *GLAI* observation on DOY 243.

A comparison between the modelled  $E$  ( $E_m$ ) and the measured  $E$  from the Bowen ratio instrumentation ( $E_{BR}$ ) shows the overall discrepancies between these values under different conditions (Fig. 4C). After the irrigation on DOY 174, there was an increase of  $E_{BR}$  to over 12 mm and an increase of  $E_m$  to over 7 mm. The  $E_m$  value appeared to be underestimated because the PROBE model does not account for the wet soil surface and adjusts the potential  $E$  at that stage for the low vegetation cover (Eq. 1). Furthermore,  $E_{BR}$  exceeded the value of  $E_p$  computed by nearby AZMET instrumentation ( $E_p$  10 mm). The same circumstances occurred for the next two irrigations on DOYs 182 and 192. However, for the latter dates, the vegetation cover was 80 % and the  $F_{GC}$  value was near 1.0, so the differences between  $E_m$  and  $E_{BR}$  were smaller.

From DOY 200 till the last irrigation (DOY 237),  $F_{GC}$  was 1.0 and the vegetation was well watered (Fig. 4D).  $F_{SW}$  was near 1.0 till DOY 245, with some declines at DOYs 168-173, 189-191 and 208-209. These declines occurred just before the next irrigation and were caused by drops in evaporation rates. Thus, the differences between  $E_m$  and  $E_{BR}$  over the period DOY 200-259 were caused primarily by the differences between  $E_{BR}$  and  $E_p$ . After the last irrigation on DOY 237,  $E_m$  decreased gradually and  $E_{BR}$  dropped dramatically. The MAD of the measured and modelled values of  $E$  for the 8 measurement days (excluding DOY 243) was 1.57 mm. The MAD for DOY 243 was large ( $E_m = 6.8$  and  $E_{BR} 2.0$  mm, MAD = 4.8 mm) because the inputs to the model did not reflect the true conditions in the field. That is, the derived *GLAI* values were erroneously high (as discussed previously), yet the leaf perforator damage was so great that the  $E_{BR}$  value was nearly zero. In response to these conflicting inputs, the PROBE model estimated  $E$  to be lower than for a potential crop, but not as low as that measured by the Bowen ratio instruments.

The comparison between the sum of modelled and measured  $E$  between irrigations is presented in Table 2.  $E_m$  values were less than  $E_{BR}$  from DOY 174-200 (because  $F_{GC} < 1.0$ ),  $E_m$  was nearly equal to  $E_{BR}$  for the period of lush, healthy growth (DOY 200-235), and  $E_m$  was greater than  $E_{BR}$  after DOY 237 when leaf perforator damage was extreme.

**Table 2.** Modelled ( $E_m$ ) and measured ( $E_{BR}$ ) cumulative evaporation over the days between irrigation events in MAC Field 116

DOY	$E_m$ , mm	$E_{BR}$ , mm
174-180	39.2	62.00
180-192	86.0	111.50
192-200	62.5	69.11
200-210	76.4	54.90
210-217	59.5	55.30
217-223	44.0	39.80
223-228	40.0	45.20
228-235	51.9	51.00
235-237	13.7	9.40

In the final stage of PROBE, the  $F_{SW}$  values calculated by the soil submodel were input into computation of  $GLAI$  and biomass in a rerun of the vegetation submodel (Eq. 5 and 6). This resulted in an increase of calculated initial  $GLAI$  value by the model and small increase of  $GLAI$  values up to DOY 190. On DOY 190,  $F_{SW}$  value dropped to 0.8 and caused a depression in the  $GLAI$  values. The  $GLAI$  curve eventually fit the observation on DOY 214. The decreases in  $GLAI$  after DOY 246 and biomass after DOY 257 were associated with no further irrigations after DOY 237 (Fig. 4E) and the decrease of  $F_{SW}$  after DOY 245 (Fig. 4D). The decrease in end-of-season biomass after implementation of the soil water submodel was nearly  $155 \text{ g}\cdot\text{m}^{-2}$ . Based on field observations made weekly at the site, this trend was more realistic than the trend exhibited in the previous iteration (Fig. 4A). The influence of  $E$  rates on the recalculation of  $GLAI$  in the vegetation submodel is readily apparent through comparison of Fig. 4a and 4e.

#### SENSITIVITY OF MODEL TO FREQUENCY AND TIMING OF $GLAI$ AND $E$ INPUTS

The PROBE model is dependent on intermittent inputs of  $GLAI$  and  $E$  from either in-situ measurements or remote sensing. To save time and money, it is best to minimise the required frequency of such inputs while maintaining high accuracy of model output. Toward this goal, we ran the model with fewer than the 9 available  $GLAI$  and  $E$  inputs, and compared the results with the field estimates of  $GLAI$  and  $E$ . The mean

absolute differences (MAD) between the n-input estimates of *GLAI* and *E* and the field estimates are summarised in Tab. 3. When the model was run with only one input value of *GLAI* and *E*, the results were poor and the MAD values were as high as 1.59 for *GLAI* and 4.63 for *E*. If the one observation of *GLAI* was early in the season, the 1-input *GLAI* estimates were underestimated. If the one observation of *GLAI* was late in the season, *GLAI* values were overestimated. For example, using single *GLAI* and *E* observations made late in the season (DOY 223, Fig. 5A) the *GLAI* simulated curve (first iteration) goes very close to the observation point on DOY 223, yet overestimates *GLAI* at the beginning of the season. The single *E* input for DOY 223 was high and resulted in a seasonal overestimation of *E* (MAD 1.59). In the next iteration of the vegetation submodel which included feedback from the soil submodel, *GLAI* and biomass were still overestimated (MAD 0.76 for *GLAI*) (Fig. 5B).

Table 3. Comparison of the results for *GLAI* and evapotranspiration estimates using a limited number of input observations. MAD is the mean absolute difference between the n-input modelled and measured values of *E* and *GLAI*

Number of observations	DOY of observation	MAD <i>GLAI</i>	MAD <i>E</i> mm-day <sup>-1</sup>
1	165	1.59	4.63
1	223	0.76	1.59
2	165 187	0.78	2.40
2	165 223	0.90	2.86
3	165 202 223	0.52	1.95
3	187 202 223	0.47	1.73
9	165 187 193 202 214 223 228 235 243	0.32	1.57

Results were similar when the model was run with only two input values (Tab. 3). However, better results were obtained when there were two observations at the beginning of the season than for one at the beginning and one late in the season. For example, with *GLAI* observations on DOY 165 and 223, the MAD for *GLAI* was 0.90. *GLAI* was underestimated at the beginning of the season, resulting in an underestimation of *E* (MAD 2.86). When two *GLAI* and *E* values were input from early in the season (e.g., DOY 165 and 187), the MAD for *GLAI* was 0.78 and MAD for *E* was 2.4.

Best results were obtained when the model was run with three inputs. Two examples are given: using inputs from DOYs 165, 202 and 223 and from DOYs 187, 202 and 223. The modelled *GLAI* curve based on observations from DOYs 165, 202 and 223 underestimated *GLAI* values from DOY 150 to 217 (Fig. 6A). On DOY 202, the derived *GLAI* value was 3.32, the 9-input modelled value was 2.95, and the 3-input modelled value was 2.60. The maximum *GLAI* value (on DOY 250) was 3.84 for the 3-input run and 3.41 for the 9-input run (on DOY 246). In this case, because of the

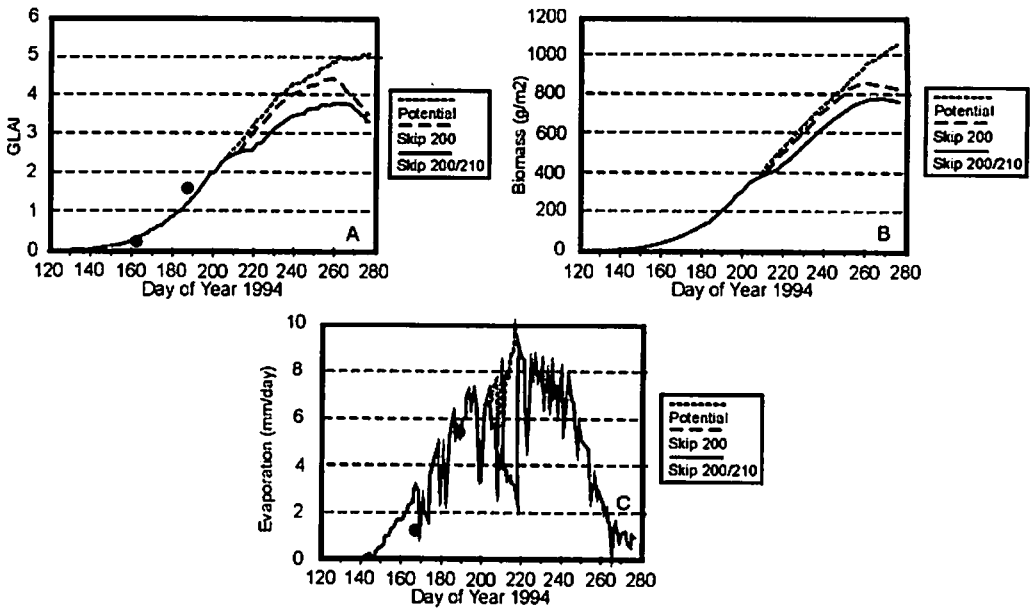


Fig. 5. A) PROBE model estimates of daily *GLAI* (bold line) from the first run of vegetation growth (VG) submodel, based on one input value of *GLAI* and *E* on DOY 223. Also included are the results based on 9 inputs (dot line). B) PROBE estimates of *GLAI* from the second iteration of the VG submodel, which included feedback from the soil water (SW) submodel

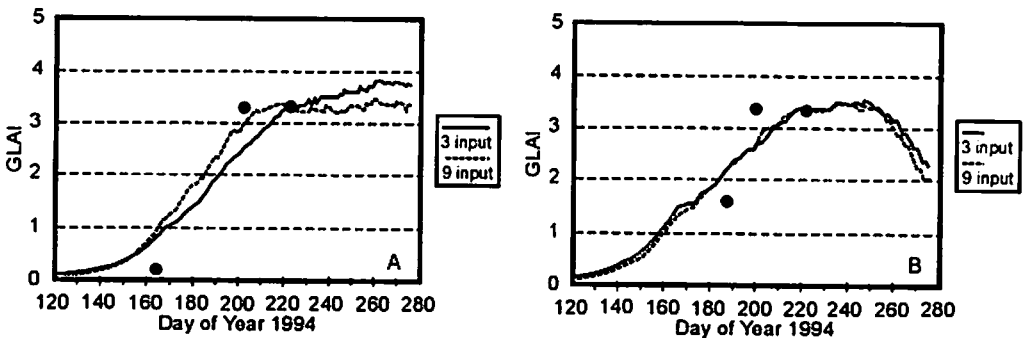


Fig. 6. PROBE model *GLAI* estimates based on three inputs (bold line) compared with results based on 9 inputs (dot line). Two examples are given: using inputs from A) DOYs 165, 202 and 223 and B) DOYs 187, 202 and 223

well-watered conditions of the growing crop, *E* values for the end of the season were the same for both the 3- and 9-input models. For this three input model, the MAD value for *GLAI* was 0.52 and for *E* 1.95. The best 3-input fit to the modelled 9-input simulation of *GLAI* was based on inputs from DOYs 187, 202 and 223 (Tab. 3). The values of *GLAI* up to DOY 173 were slightly overestimated, but after this time, the values matched very well (Fig. 6B). The MAD value was 0.47 for *GLAI* and 1.73 for

*E*. The overestimation of *GLAI* at the beginning of the season gave higher biomass values, which at the maximum (DOY 255) differed from the 9-input value by  $105 \text{ g}\cdot\text{m}^{-2}$ . The difference in *GLAI* value at the maximum, which was at the DOY 246, was 0.12.

## SENSITIVITY OF MODEL TO ACCURACY OF OBSERVED *GLAI* VALUES

The PROBE model output will undoubtedly be affected by the accuracy of the intermittent inputs of *GLAI* and *E*. To test this sensitivity, we computed the standard deviation (*sd*) of the *GLAI* measurements based on our multiple samples from selected fields for each day and ran the model under two conditions: 1) for inputs of *GLAI* minus one *sd* (*GLAI* - 1*sd*) and 2) for inputs of *GLAI* plus one *sd* (*GLAI* + 1*sd*). For *GLAI* - 1*sd*, the *GLAI* inputs ranged from 0.18 (DOY 165) to 3.49 (DOY 193) with a value of 2.83 from DOY 202 to 243. In this PROBE run, the  $F_{GC}$  factor was less than 1 for the entire growing season. It resulted in an underestimation of *E* values, with a MAD between modelled and measured *E* of 1.90 mm. The evaporation rate on DOY 170 declined to the value of 2.0 and  $F_{SW}$  was 0.7, resulting in a decrease in biomass of  $160 \text{ g}\cdot\text{m}^{-2}$ .

For condition 2 (*GLAI* + 1*sd*), the *GLAI* inputs ranged from 0.22 (DOY 165) to 4.3 (DOY 193) with a value of 3.81 from DOY 202 to 243. The vegetation submodel was influenced by the high *GLAI* input on DOY 193; thus, the slope of the *GLAI* curve was very steep until DOY 193, followed by decline to the value of 3.81 on DOY 202. In this case, the parameter, which controls the leaf lifespan was reinitialised by the model to be low. Thus, the modelled biomass declined to zero on DOY 205.

## BIOMASS FORECASTING AND IRRIGATION SCHEDULING USING PROBE

The PROBE model may prove useful for biomass forecasting and irrigation scheduling. To investigate this application, we ran PROBE for a hypothetical date in the middle of the season for which the user had only early-season information on *E* and *GLAI* and was trying to determine the time of next irrigation. That is, the growing season was assumed to be from DOY 120-275, the user had only the first two observations of *GLAI* and *E* on DOYs 165 and 187, and irrigations had already been applied on DOYs 147, 174, 180 and 192. The hypothetical date that this simulation was run was DOY 193 and the hypothetical farm manager was trying to schedule the next irrigations.

In scenario one (dot line, Fig. 7A), irrigations were scheduled for DOYs 200, 210, 217, 223, 228, 235 and 237 (as actually applied to Field 116) and the crop grew at the potential rate (where  $F_{SW} = 1.0$  throughout the season). In scenario two (dashed line), the irrigation on DOY 200 was skipped and, in scenario three (bold line), the irrigations on DOYs 200 and 210 were skipped. For scenario two, *E* decreased to below 3.0

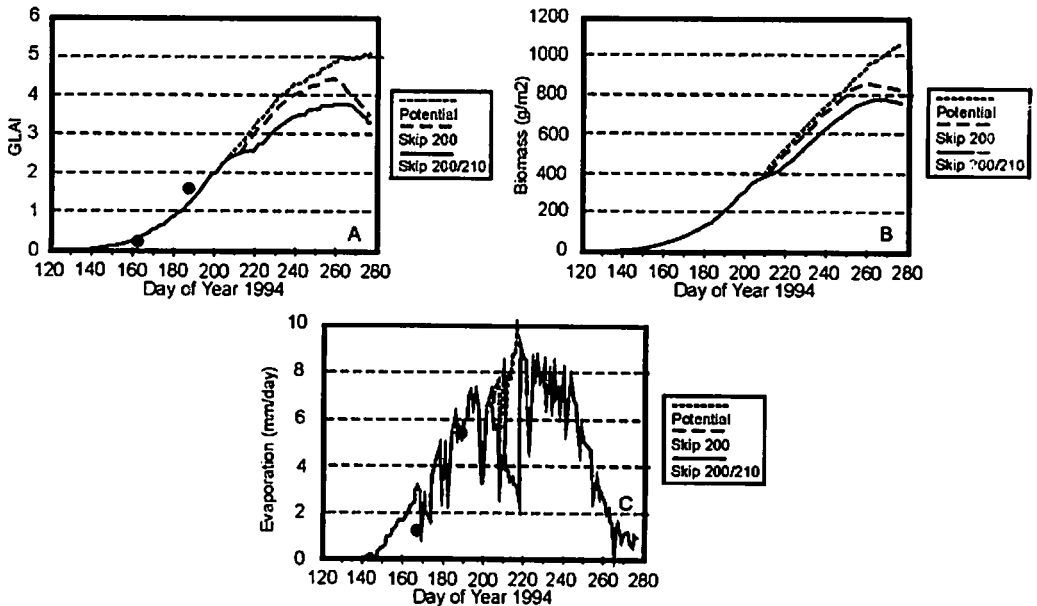


Fig. 7. A) PROBE estimates of *GLAI* based on 2 inputs of *GLAI* and *E* (solid dots) with irrigations on all nine days (dot line), skipping the irrigation on DOY 200 (dashed line) and skipping the irrigation on DOYs 200 210 (bold line). B) PROBE biomass estimates for same scenario as Fig. 7A. C) PROBE evaporation estimates for same scenario as Fig. 7A

mm just after DOY 200 (Fig. 7B).  $F_{SW}$  dropped from 1.0 to 0.6 and there was a steady decline in *E* until the next irrigation on DOY 210. In this scenario, the *GLAI* values did not regain the potential level. On DOY 256, the maximum value of *GLAI* was lower ( $GLAI = 4.42$ ) than for scenario one ( $GLAI = 4.84$ ). Due to the decrease of  $F_{SW}$  after DOY 246, biomass decreased by over  $100 \text{ g}\cdot\text{m}^{-2}$  on DOY 260.

In scenario three (skipping irrigations on DOYs 200 and 210), *E* dropped below 3 mm, (Fig. 7C), resulting in a large drop in  $F_{SW}$  and a large difference in *GLAI* values compared to the potential (Fig. 7A). The maximum value of *GLAI* was 3.8 on DOY 259 and the maximum biomass on DOY 265 was  $775 \text{ g}\cdot\text{m}^{-2}$  ( $225 \text{ g}\cdot\text{m}^{-2}$  lower than the biomass estimated for scenario one).

## DISCUSSION AND CONCLUSIONS

The design of the PROBE model with interactive soil and vegetation submodels results in several advantages for crop growth simulation. First, the input of *E* into the second run of the vegetation growth model resulted in much improved estimates of *GLAI* and biomass. Second, the model has potential for such applications as irrigation scheduling, since it gives the user both information on water loss to date and on potential crop growth based on future irrigations. Finally, the iterative tuning of model

parameters based on periodic inputs of *GLAI* and *E* allows the model to be both simple (requiring few inputs) and accurate. Since there is evidence that both *GLAI* and *E* can be estimated with remotely sensed data (MORAN *et al.*, 1995), there is also potential for the PROBE model to be applied over large areas in a Geographic Information System (GIS).

The work presented here investigated the frequency, timing and precision of model inputs required maintaining output accuracy. Results showed that accurate estimates of daily *E*, *GLAI* and biomass could be obtained with only three inputs of *GLAI* and *E* during the cotton growing season. However, the timing of these three measurements was crucial. Based on our analysis, the optimal times for model inputs of *GLAI* and *E* would be early in the season (e.g., between DOY 165 or 187), near the time of maximum flowering (e.g., DOY 202), and near the time of maximum green bolls (e.g., DOY 223). The latter two times are critical because the dates of maximum flowering and maximum green bolls have some influence on the future cotton yield.

The PROBE estimates of daily *GLAI*, biomass and *E* were very sensitive to the precision of the periodic *GLAI* and *E* measurements that were used as input. A variation of one standard deviation in *GLAI* values resulted in an average underestimation of *E* values by 1.9 mm. Errors of this magnitude are unacceptable for use in scheduling crop irrigations.

Overall, the modelled and measured values of *E* corresponded well, particularly when the crop fully covered the ground. The largest differences between  $E_m$  and  $E_{BR}$  values were not necessarily due to weaknesses in the model, but rather to discrepancies between the definitions of  $E_m$  and  $E_{BR}$  and discrepancies between  $E_{BR}$  and the AZMET-derived values of potential *E* ( $E_p$ ). By definition in Eq. (1),  $E_m$  can't equal  $E_p$  before the crop reaches full vegetative cover because  $F_{GC}$  will be less than 1.0; thus, there will be occasions (e.g., when the field is flooded and the crop is immature) when  $E_{BR}$  will equal  $E_p$ , and  $E_m$  could be close to zero. Furthermore, it was common for the  $E_{BR}$  estimates to exceed  $E_p$  computed from the AZMET meteorological data, resulting in discrepancies between  $E_{BR}$  and  $E_m$  even when the vegetation fully covered the soil surface.

A weakness in PROBE became apparent at the end of the cotton season when the leaf perforator infestation was particularly devastating. The model assumed controlled leaf senescence based on input information regarding the *GLAI* and *E* measurements and the last date of irrigation. Toward the end of the cotton growth in Field 116, the derived estimates of *GLAI* was still high and the field was recently irrigated, but the  $E_{BR}$  measurement indicated that the plants had stopped transpiring due primarily to insect damage. With this conflicting information, PROBE estimates of  $E_m$  were too high for the end of the season. The model logic could be refined to account for such catastrophic conditions.

## ACKNOWLEDGEMENTS

The large part of the work has been done during Fulbright scholarship of Polish author in USDA – ARS Water Conservation Laboratory. Work at MAC was accomplished with the cooperation and expertise of the resident farm managers and staff of the Univ. of Ariz. Maricopa Agricultural Centre, particularly Roy Rauschkolb, Bob Roth, Pat Murphree and Mac D Hartman. We also acknowledge the daily efforts of the technicians from the U.S. Water Conservation Laboratory in all aspects of the field work and subsequent data archival and analysis: Robert La Morte, Ron Seay, Mike Baker, Lynnette Eastman, Stephanie Johnson, Ric Rokey, Ed Perry, Leslie Smith and Faiz Rahman.

## REFERENCES

1. ARKIN G.F., VANDERLIP, WIEGAND C.L., HUDDLESTON H., 1977. The future role of a crop model in large area yield estimation. In Proceedings of the Crop Modelling Workshop, USDC-NOAA-EDIS-CEAS, Columbia, MO p. 87-116.
2. BROWN K.W., 1969. A model of the photosynthesizing leaf. *Physiologia Plantarum* 22 p. 620-637.
3. BROWN P.J., 1989. Accessing the Arizona Meteorological Network by Computer. The University of Arizona, Tucson, AZ 85721.
4. CHARLES-EDWARDS D.A., DALEY D., REMINGTON G.M., 1986. Modeling Plant Growth and Development. Orlando: Academic Press FL. 235 pp.
5. FEDDES R.A., KOWALIK P.J., ZARADNY H., 1978. Simulation of field water use and crop yield. Wageningen: Centre for Agricultural Publishing and Documentation 189 pp.
6. HODGES T., KANEMASU E.T., 1977. Modelling daily dry matter production of winter wheat. *Agronomy Journal* 69 p. 974-978.
7. MAAS S.J., 1992. GRAMI: A crop growth model that can use remotely sensed Information ARS91. U.S. Dept. of Agric., Washington, DC, 78 pp.
8. MAAS S.J., 1993a. Parameterized model of gramineous crop growth: I. Leaf area and dry mass simulation. *Agronomy Journal* 85 p. 348-353.
9. MAAS S.J., 1993b. Parameterized model of gramineous crop growth: II within – season simulation calibration, *Agronomy Journal* 85 p. 354-358.
10. MAAS S.J., JACKSON R.D., IDSO S.B., PINTER P.J. Jr., REGINATO R.J., 1989. Incorporation of remotely sensed indicators of water stress in a crop growth simulation model. Preprints 19th Conference on Agricultural and Forest Meteorology, 7-10 March 1989, Charleston, SC, American Meteorological Society, Boston, MA, p. 228-231.
11. MAAS S.J., MORAN M.S., JACKSON R.D., 1992. Combining remote sensing and modelling for regional resource monitoring. Part II: A simple model for estimating surface evaporation and biomass production. Proc. ASPRS/ASPRS/ACSM/RT92, Wash. DC, 3-7 Aug. 1992, p. 225-234.
12. MORAN M.S., CLARKE T.R., QI J., PINTER P.J. Jr., 1996. MADMAC: A test of multispectral airborne imagery as a farm management tool. Proc. 26th Intern. Symp. on Rem. Sens. Env., 25-29 March, Vancouver, BC, Canada, p. 612-617.
13. MORAN M.S., MAAS S.J., PINTER P.J. Jr., 1995. Combining Remote Sensing and Modeling for Estimating Surface Evaporation and Biomass Production, *Remote Sensing Reviews* 12 p. 335-353.
14. RITCHIE J.T., BURNETT E., 1971. Dryland evaporative flux in a subhumid climate. II. Plant influences. *Agronomy Journal* 63 p. 56-62.

15. ROSENTHAL W.D., ARKIN G.F., SHOUSE P.J., JORDAN W.R., 1987. Water deficit effects on transpiration and leaf growth, *Agronomy Journal* 79 p. 1019-1026.
16. Van BAVEL C.H.M., 1966. Potential evaporation: The combination concept and its experimental verification. *Water Resources Research* 2 p. 455-467.
17. WIT C.T. de, BROUWER R., PENNING de VRIES F.W.T., 1970. The simulation of photosynthetic systems. Prediction and measurement of photosynthetic productivity. I. Setlic (Ed). Pudoc, Wageningen, The Netherlands 148 pp.
18. WIT C.T. de, Van KEULEN H., 1987. Modelling production of field crops and its requirements. *Geoderma* 40 p. 254-265

## STRESZCZENIE

### Modelowanie wzrostu roślin i terminu nawodnień z zastosowaniem teledetekcji

Słowa kluczowe: *model PROBE, ewaporacja, GLAI, bilans wody w glebie, prognozowanie wzrostu roślin*

PROtotypowy model Biomasy i Ewapotranspiracji (PROBE) został utworzony do symulacji dziennego przyrostu biomasy ( $B$ ) i ewapotranspiracji ( $E$ ) dla naturalnych roślinnych ekosystemów (MASS *et al.*, 1992). Danymi wejściowymi do modelu są podstawowe dane meteorologiczne i okresowe dane wskaźnika powierzchni zielonej liści ( $GLAI$ ) oraz ewapotranspiracji  $E$ . Danymi wyjściowymi są codzienne wartości  $GLAI$ ,  $E$ , biomasa i wilgotność gleby. Model składa się z dwóch submodeli. Pierwszy dotyczy wzrostu roślin, drugi – bilansu wodnego gleby, w którym symulowana wartość  $GLAI$  z submodelu pierwszego wpływa na obliczenie ewapotranspiracji w submodelu drugim. Następnie symulowana wartość  $E$  wpływa na ostateczną symulację  $GLAI$ . W wyniku pracy model został skalibrowany dla bawełny dla całego okresu wzrostu uprawy, a następnie modelowane wartości  $GLAI$  i  $E$  zostały porównane z wartościami uzyskanymi z badań terenowych. W wyniku symulacji modelu została określona dokładność wyznaczenia  $GLAI$  i  $E$  w zależności od częstotliwości, okresu i precyzji wyników  $GLAI$  i  $E$  uzyskanych teledetekcyjnie. Została zbadana przydatność tego modelu do prognozy wielkości biomasy i terminu nawodnień.

Received 25.09.2000

Reviewers:

*Prof. Piotr Kowalik*

*Assistant prof. Leszek Łabędzki*